

## Electronic Supplementary Information

Iron L<sub>3</sub>-edge energy shifts for the full range of possible 3d occupations within the same oxidation state of iron halides

Max Flach,<sup>a,b</sup> Konstantin Hirsch,<sup>a</sup> Martin Timm,<sup>a</sup> Olesya S. Ablyasova,<sup>a,b</sup> Mayara da Silva Santos,<sup>a,b</sup> Markus Kubin,<sup>a</sup> Christine Bülow,<sup>a,b</sup> Tim Gitzinger,<sup>a,b</sup> Bernd von Issendorff,<sup>b</sup> J. Tobias Lau,<sup>a,b,\*</sup> and Vicente Zamudio-Bayer<sup>a</sup>

<sup>a</sup> *Abteilung für Hochempfindliche Röntgenspektroskopie, Helmholtz-Zentrum Berlin für Materialien und Energie, Albert-Einstein-Str. 15, 12489 Berlin, Germany.*

<sup>b</sup> *Physikalisches Institut, Albert-Ludwigs-Universität Freiburg, Hermann-Herder-Str. 3, 79104 Freiburg, Germany.*

\**E-mail: tobias.lau@helmholtz-berlin.de*

# 1 Sample preparation

## 1.1 Electrospray ionisation source

Commercially available salts (see table S1) are dissolved in methanol or water as solvents to obtain solutions with a concentration of  $\approx 1$  mmol/L. The solution is sprayed at a flowrate of 0.25 ml/h.

Salt	purity	CAS
Fe(II)I <sub>2</sub> (anhydrous)	min 97%	7783-86-0
Fe(II)Br <sub>2</sub> (anhydrous)	min 98%	7789-46-0
Fe(II)Cl <sub>2</sub> (anhydrous)	min 99,5%	7758-94-3
Fe(III)F <sub>3</sub> (anhydrous)	min 97%	7783-50-8

Table S1: Compilation of chemicals used in sample preparation. All samples were purchased from *Alfa Aesar*.

## 1.2 Magnetron sputter source

Fe<sup>+</sup> cations also used as a precursor for FeCl<sup>+</sup> production are generated by argon sputtering of an iron target. For FeCl<sup>+</sup> production, iron ions are exposed to CH<sub>2</sub>Cl<sub>2</sub> gas in a collision cell at a pressure of  $\approx 10^{-4}$  mbar. FeCl<sup>+</sup> is subsequently isolated using a quadrupole mass filter.

# 2 Data treatment

All data sets were acquired at the UE52PGM Ion Trap setup [1] with a bandwidth of 80 meV (step size 0.03 eV) for the high resolution spectra and 200 meV (step size 0.08 eV) for the overview spectra.

For consistency across different samples only partial ion yield of Fe<sup>2+</sup> product ions are considered. We, however, also checked the partial ion yield of all other photo ions to be proportional to Fe<sup>2+</sup>. Hence, the presented data is proportional to the total ion yield and therefore also to the X-ray absorption.

## 2.1 Energy calibration

In order to account for photon energy drift over time, the energy in all scans was sequentially referenced after acquisition to one FeCl<sup>+</sup> scan of high signal-to-noise ratio. The latter was acquired right after energy calibration during commissioning of the beamline.

## 2.2 Averaging procedure and error estimation

To improve the signal-to-noise ratio, multiple scans of the same sample were averaged after single scan referencing for energy calibration, using linear interpolation. The total uncertainty  $\Delta E_{\text{total}}$  was obtained through error propagation taking into account the uncertainties of beamline ( $\Delta E_1$ ), sample ( $\Delta E_2$ ) and reference ( $\Delta E_3$ ) scan reproducibility, and of the sequential referencing during analysis ( $\Delta E_4$ ).

System	$\Delta E_1/\text{eV}$	$\Delta E_2/\text{eV}$	$\Delta E_3/\text{eV}$	$\Delta E_4/\text{eV}$	$\Delta E_{\text{total}}/\text{eV}$
Fe <sup>+</sup>	$\pm 0.014$	$\pm 0.018$	$\pm 0.003$	$\pm 0.030$	$\pm 0.037$
FeF <sup>+</sup>	$\pm 0.014$	$\pm 0.019$	$\pm 0.011$	$\pm 0.030$	$\pm 0.040$
FeCl <sup>+</sup>	$\pm 0.014$	$\pm 0.0$	$\pm 0.003$	$\pm 0.030$	$\pm 0.033$
FeBr <sup>+</sup>	$\pm 0.014$	$\pm 0.025$	$\pm 0.006$	$\pm 0.030$	$\pm 0.042$
FeI <sup>+</sup>	$\pm 0.014$	$\pm 0.027$	$\pm 0.011$	$\pm 0.030$	$\pm 0.044$

Table S4: Table of error contributions of the measured samples and the resulting total error.

### 3 Charge transfer multiplet calculations

The calculated spectra were shifted to fit the energy position of the experimental data by the amounts shown in table S5.

System	$\Delta$ /eV	$U_{dd}$ /eV	$U_{pd}$ /eV	T1 /eV	T2 /eV	T3 /eV	T4 /eV	d occupation /e	shifted by /eV
FeF <sup>+</sup>	0.5	0.5	0	0.5	0.5	0.5	0.5	6.132	-0.68
FeCl <sup>+</sup>	-0.1	0.5	0	0.5	0.5	0.5	0.5	6.261	-1.01
FeBr <sup>+</sup>	-0.5	0.5	0	0.5	0.5	0.5	0.5	6.2584	-1.03
FeI <sup>+</sup>	-2	0	0.5	0.5	0.7	0.8	0.6	6.5962	-0.63

Table S5: Parameters of the charge transfer multiplet calculations (using CTM4XAS code [2]) shown in the main text of the paper in fig. 1 and the resulting 3d occupation of FeX<sup>+</sup>.

### 4 Turbomole density functional theory (DFT)

The Turbomole DFT calculation were done with the B3LYP functional and the def2-TZVP basis set, with the iron 3d orbital population derived by natural population analysis, after a geometry optimization was performed. [3]

System	Fe 3d(tot.)/e
FeF <sup>+</sup>	6.34
FeCl <sup>+</sup>	6.53
FeBr <sup>+</sup>	6.57
FeI <sup>+</sup>	6.73

Table 4: Natural populations of iron 3d derived from Turbomole DFT calculations.

### 5 Electronegativities

All electronegativities  $\chi$  were determined from ionization energies (IE) and electron affinities (EA) according to Mulliken [4].

Element	IE/eV [5]	EA/eV	$\chi$ /eV
F	17.42282	3.448 [6]	10.43541
Cl	12.967633	3.613 [6]	8.2903165
Br	11.81381	3.363 [6]	7.588405
I	10.451260	3.063 [6]	6.75713

Table S6: Compilation of first ionization energies and electron affinities for all halogens. Electronegativities are determined according to Mulliken [4].

## 6 Overview spectra

In addition to the high resolution spectra of the iron  $L_3$ -edge, we also measured overview spectra of the iron  $L_{2,3}$ -edge (see figure S1).

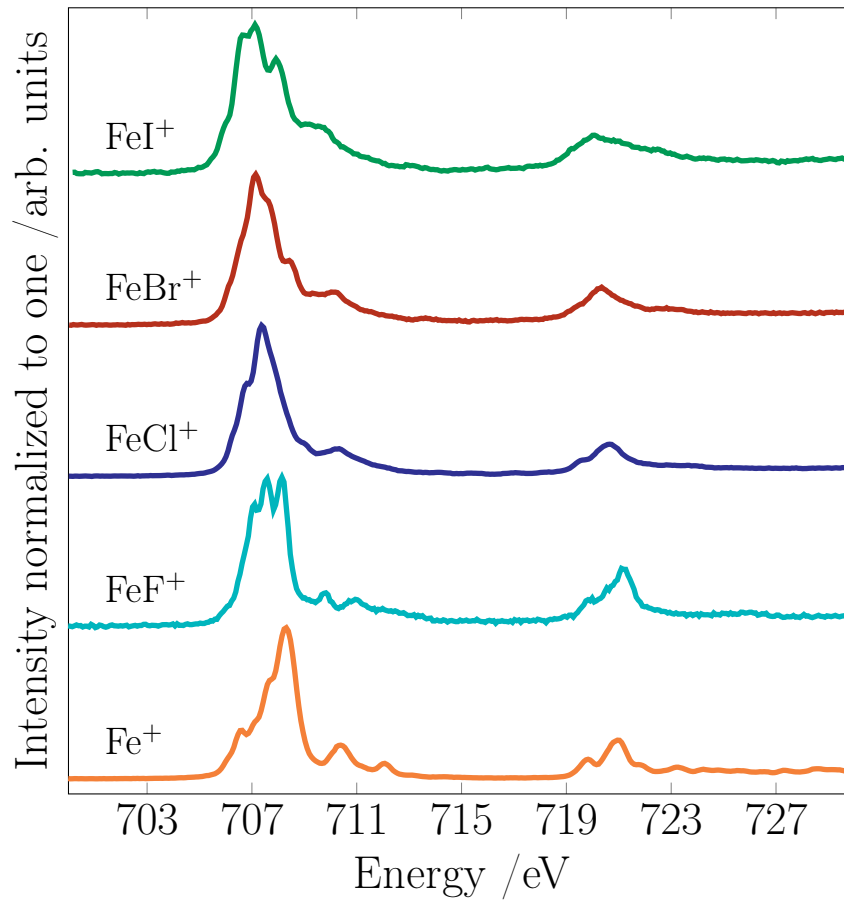


Figure S1: Overview spectra  $\text{FeX}^+$  Iron  $L_{2,3}$ -edge measured with a bandwidth of 200 meV and step size of 0.08 eV.

## References

- [1] K. Hirsch et al. “X-ray spectroscopy on size-selected clusters in an ion trap: from the molecular limit to bulk properties”. In: *Journal of Physics B: Atomic, Molecular and Optical Physics* 42.15 (2009), p. 154029.
- [2] Eli Stavitski and Frank M.F. de Groot. “The CTM4XAS program for EELS and XAS spectral shape analysis of transition metal L edges”. In: *Micron* 41.7 (2010), pp. 687–694.
- [3] Malte Von Arnim and Reinhart Ahlrichs. “Performance of parallel TURBOMOLE for density functional calculations”. In: *Journal of Computational Chemistry* 19.15 (1998), pp. 1746–1757.
- [4] Robert S. Mulliken. “A New Electroaffinity Scale; Together with Data on Valence States and on Valence Ionization Potentials and Electron Affinities”. In: *The Journal of Chemical Physics* 2.11 (1934), pp. 782–793.
- [5] A. Kramida et al. NIST Atomic Spectra Database (ver. 5.8), [Online]. Accessed: [2021, September 27]. National Institute of Standards and Technology, Gaithersburg, MD. 2020.
- [6] R. Stephen Berry and Curt W. Reimann. “Absorption Spectrum of Gaseous F- and Electron Affinities of the Halogen Atoms”. In: *The Journal of Chemical Physics* 38.7 (1963), pp. 1540–1543.